https://doi.org/10.1016/j.engstruct.2020.111613

A PEM-based topology optimization for structures subjected to stationary random excitations

Xuqi Zhao[a], Baisheng Wu[a], Siu-Kai Lai[b,c,*], Zhengguang Li[d], Huixiang Zhong[a]

[a] *School of Electro-Mechanical Engineering, Guangdong University of Technology, Guangzhou 510006, PR China*

[b] *Department of Civil and Environmental Engineering, The Hong Kong Polytechnic University, Hung Hom, Kowloon, Hong Kong, PR China*

[c] *Hong Kong Branch of National Rail Transit Electrification and Automation Engineering Technology Research Center, The Hong Kong Polytechnic University, Kowloon, Hong Kong, PR China*

[d] *School of Mathematics, Jilin University, Changchun 130012, PR China*

Abstract

This paper focuses on the topological optimization of structures subjected to stationary random excitations. A new topology optimization scheme based on the pseudo excitation method (PEM) for calculating structural random responses in a frequency domain is proposed. In this method, the Sturm sequence is applied to adaptively determine the number of lower-order modes used for mode superposition analysis. The contribution of unknown higher-order modes is approximated by the partial sum of a constructed convergent series. Since the method can offer an approximate expression of structural response solutions, not only it can enhance the flexibility of implementation and also improve the computational effort and accuracy. In addition, derivatives of the objective function are derived by means of the adjoint method. They can be achieved by solving an adjoint problem that is similar to the original governing equation of the system. Two illustrative examples are presented to affirm the proposed scheme in terms of computational accuracy and efficiency.

Keywords: Topology optimization, Stationary random excitation, Pseudo excitation method, Adaptive algorithm

* Corresponding author.

E-mail address: sk.lai@polyu.edu.hk (S.K. Lai)

1. Introduction

Structural topology optimization is a method to find the best way for shape configuration and material distribution within a design domain [1]. Various topology optimization methods have been widely applied to structural design under static loads [2]. However, structural responses under dynamic effects in real-life engineering conditions are a major concern [3]. Hitherto, dynamic topology optimization problems, including structural natural frequencies [4, 5], transient responses [6, 7] and steady-state responses [8-10], have been extensively investigated. In engineering applications, random factors are often encountered in structural design problems [11], such as stochastic parameters [12], and uncertainties in stiffnesses, boundaries and loads [13-15]. One of these crucial topics is the design of engineering structures under stationary random excitations [16] (e.g., parametric size optimization problems [17-20]), but there are only few studies on the topology optimization of stochastically excited structures due to the inherent complexity of such problems, including the computation of structural responses and its corresponding sensitivities. Rong et al. [21, 22] studied the topological optimum design of structures under random response constraints based on the evolutionary structural optimization method. Zhang et al. [23] investigated the integrated layout optimization of multi-component structures under static loads and random excitations using the density method. In addition, the complete quadratic combination (CQC) method [24] was used to obtain the structural responses of this problem but requires a high computational effort.

Recently, many researchers have devoted to studying the topology optimization of large-scale structures subjected to random excitations. For example, Zhang et al. [25] proposed a computational scheme for topology optimization by combining the PEM [26] along with the mode acceleration method (MAM) [27]. They achieved a much better optimization configuration than those obtained by the conventional type of the PEM. Based on this idea of computing structural responses, Zhao et al. [28] proposed a topology optimization procedure with dynamic stress response constraints under stationary random excitations. However, the computational efficiency and accuracy of structural responses and sensitivity analysis can be greatly affected by the number of lower-order modes involved [29]. Zhu et al. [30] applied a topology optimization method to design a frame structure under linear stationary stochastic excitations. Yang et al. [31] further utilized the solid isotropic

material penalization (SIMP) method to conduct the topology optimization of structures subjected to stochastic filtered white noise excitations. In these two studies, they obtained the values of objective functions through modal truncations and performed the calculation of eigenvector derivatives for sensitivity analysis.

However, computing the derivatives of eigenvectors, especially those with repeated eigenvalues, is a complicated topic [32, 33]. Although the computational cost of objective function values and eigenvector derivatives based on the modal superposition method is low, the results are generally inaccurate due to the insufficient contribution of higher-order modes [34]. To circumvent this deficiency, Gomez and Spencer [29] proposed a topology optimization framework for structures subjected to stationary stochastic dynamic loads. More recently, they [35] further extended the framework to study the topology optimization of buildings under stochastic base excitations. These two studies obtained the covariance of responses by solving the Lyapunov equation [36], which is a parallel work along with the frequency- and time-domain approaches. For large-scale engineering problems, solving the Lyapunov equation can be resorted to the use of vectorization and Kronecker product techniques [37].

Generally, the optimization process involves a series of structural analysis responses. Besides, the sensitivity analysis based on the adjoint method requires solving a set of governing equations similar to that of structural responses. Therefore, the accuracy and efficiency of calculation methods for structural responses are two critical points for structural topology optimization problems. Meanwhile, various design variables of structures may change at each iteration step of topology optimization, such that the adaptability of computational methods is equally important.

In this paper, we propose a PEM-based approach to deal with the topology optimization of large-scale structures under stationary random excitations. The method considers the power spectral density (PSD) of random displacements over a wide frequency interval as an objective function. In addition, a set of linear dynamic systems with proportional damping and their structural responses under stationary random excitations are also considered. In the proposed scheme, the new method (NM) [38] for frequency responses and the PEM [26] for random responses are integrated to compute frequency domain solutions in a wide frequency interval. The Sturm sequence is first

applied to adaptably determine the number of lower-order modes required for modal superposition. This is a crucial step because the structural modes may change when updating the design variables. A partial sum of a convergent series is then constructed to approximate the contribution of unknown higher-order modes. By using an iterative method to determine the response at the highest excitation frequency, the number of terms in the sum can be determined adaptively. The resulting expression of the frequency response is valid throughout the frequency interval of interest. The calculation process is simple and low-cost. For multi-input cases, one only needs to perform the iteration algorithm under different loads to construct a new convergent series without any extra modal analysis. The topology optimization of structures under stationary random excitations is then performed. The integral of the PSD of certain user-defined degrees of freedom (DOFs) in these structures over a frequency interval is considered as an objective function. Derivatives of this objective function are obtained by using the adjoint method, where the adjoint vectors can be solved by the method recently proposed by the authors [38].

The rest of this paper is organized as follows. Section 2 introduces a PEM-based method for the analysis of structures subjected to stationary random excitations in a frequency interval. A calculation method for frequency responses is also provided. In Section 3, the formulation of topology optimization and the sensitivity analysis based on the adjoint method are both reviewed, where the optimization procedures can be put forward. Two illustrative examples are presented to demonstrate the accuracy and efficiency of the proposed scheme in Section 4. Finally, the major findings of this work are concluded in Section 5.

2. Problem formulation

A discretized multi-degree-of-freedom structural system subjected to stationary random excitations can be written as

$$\mathbf{M}\ddot{\mathbf{X}}(t)+\mathbf{C}\dot{\mathbf{X}}(t)+\mathbf{K}\mathbf{X}(t)=\mathbf{B}\mathbf{f}(t) \tag{1}$$

where $\mathbf{K}$ and $\mathbf{M}$ are the large and sparse $n\times n$ symmetric positive definite stiffness and mass matrices, respectively; $\mathbf{C}$ is the proportional damping matrix, i.e., $\mathbf{C}=\alpha\mathbf{M}+\beta\mathbf{K}$ where α and β are two real scalars; $\mathbf{X}(t)$, $\dot{\mathbf{X}}(t)$ and $\ddot{\mathbf{X}}(t)$ denote the n-dimensional displacement, velocity

and acceleration vectors of the system, respectively; $\mathbf{B}$ is an $n\times d$ load effect matrix that represents the excitation distribution; and $\mathbf{f}(t)$ is a d-dimensional stationary random excitation vector, whose PSD matrix is denoted by $\mathbf{S}_f(\omega)$.

The input and output PSD matrices $\mathbf{S}_f(\omega)$ and $\mathbf{S}_x(\omega)$ are given by [24]

$$\mathbf{S}_x(\omega)=\bar{\mathbf{H}}(\omega)\mathbf{B}\mathbf{S}_f(\omega)\mathbf{B}^{\mathrm{T}}\mathbf{H}^{\mathrm{T}}(\omega) \tag{2}$$

where $\mathbf{H}(\omega)$ is a complex frequency response matrix, that is

$$\mathbf{H}(\omega)=\left(\mathbf{K}+i\omega\mathbf{C}-\omega^2\mathbf{M}\right)^{-1}=\mathbf{\Phi}\left[\mathbf{\Lambda}+i\omega\left(\alpha\mathbf{I}+\beta\mathbf{\Lambda}\right)-\omega^2\mathbf{I}\right]^{-1}\mathbf{\Phi}^{\mathrm{T}}. \tag{3}$$

In Eqs. (2) and (3), $\bar{\mathbf{H}}(\omega)$ is the complex conjugate of $\mathbf{H}(\omega)$, $\mathbf{\Phi}=\left[\boldsymbol{\varphi}_1,\boldsymbol{\varphi}_2,...,\boldsymbol{\varphi}_n\right]$, $\mathbf{\Lambda}=\mathrm{diag}\left(\omega_1^2,\omega_2^2,...,\omega_n^2\right)$ and $\mathbf{I}$ is an $n\times n$ unity matrix. Here, $\boldsymbol{\varphi}_j$ and ω_j $\left(j=1,2,...,n\right)$ are the eigenvectors and eigenfrequencies of the corresponding undamped system, respectively. They satisfy

$$\begin{cases}\mathbf{K}\boldsymbol{\varphi}_i=\omega_i^2\mathbf{M}\boldsymbol{\varphi}_i\\ \boldsymbol{\varphi}_j^{\mathrm{T}}\mathbf{M}\boldsymbol{\varphi}_i=\delta_{ij}\end{cases}\ i,j=1,2,...,n \tag{4}$$

where δ_{ij} is the Kronecker delta and ω_i is the frequency (rad/s).

The CQC method [24] can be used to compute the approximate PSD matrix of random displacement responses in Eq.(2) by using the modal truncation method. However, the calculation cost is relatively high for the case where the number of modes used in the CQC method is large. To reduce the computational effort, the cross-correlation terms between the participant modes are usually neglected in Eq.(2) [24]. This is acceptable only for the case that a structure is slightly damped and the eigenfrequencies of the structure can be well separated. To overcome this deficiency, Lin et al. [26] proposed a fast CQC method (named as the PEM) to improve the computational efficiency which does not follow the traditional procedures. The main idea of the PEM is to compute Eq.(2) by means of the multiplication of vectors instead of matrices.

2.1 Pseudo excitation method

The PSD matrix $\mathbf{S}_f(\omega)$ of a multi-input stationary random excitation $\mathbf{f}(t)$ is a non-negative

definite Hermitian matrix and can be decomposed into the following form [26]

$$\mathbf{S}_f(\omega)=\sum_{m=1}^{q}\lambda_m\mathbf{u}_m\overline{\mathbf{u}}_m^{\mathrm{T}}=\sum_{m=1}^{q}\overline{\boldsymbol{\gamma}}_m\boldsymbol{\gamma}_m^{\mathrm{T}} \tag{5}$$

where q is the rank of the matrix $\mathbf{S}_f$, λ_m and $\mathbf{u}_m$ are the eigenvalue and eigenvector of $\mathbf{S}_f$, respectively. The vector $\boldsymbol{\gamma}_m$ is defined as $\boldsymbol{\gamma}_m$ □ $\sqrt{\lambda_m}\overline{\mathbf{u}}_m$. Substituting Eq.(5) into Eq.(2) yields

$$\mathbf{S}_x(\omega)=\sum_{m=1}^{q}\overline{\left[\mathbf{H}(\omega)\mathbf{B}\boldsymbol{\gamma}_m\right]}\left[\mathbf{H}(\omega)\mathbf{B}\boldsymbol{\gamma}_m\right]^{\mathrm{T}}. \tag{6}$$

Consider a linear system, the PSD matrix $\mathbf{S}_x(\omega)$ of random displacement responses can be computed by a harmonic response analysis. The exact responses of Eq.(6) can be obtained by using a full method (FM) to solve the complex algebraic equations at each interested frequency point, but this leads to a huge computational effort. Therefore, the expression of Eq.(6) is approximated by using a modal truncation as follows:

$$\mathbf{S}_x(\omega)\approx\sum_{m=1}^{q}\overline{\left[\mathbf{H}_{n_d}(\omega)\mathbf{B}\boldsymbol{\gamma}_m\right]}\left[\mathbf{H}_{n_d}(\omega)\mathbf{B}\boldsymbol{\gamma}_m\right]^{\mathrm{T}} \tag{7}$$

where $\mathbf{H}_{n_d}(\omega)=\boldsymbol{\Phi}_{n_d}\left[\boldsymbol{\Lambda}_{n_d}+i\omega\left(\alpha\mathbf{I}_{n_d}+\beta\boldsymbol{\Lambda}_{n_d}\right)-\omega^2\mathbf{I}_{n_d}\right]^{-1}\boldsymbol{\Phi}_{n_d}^{\mathrm{T}}$, $\boldsymbol{\Phi}_{n_d}$ and $\boldsymbol{\Lambda}_{n_d}$ are the n_d lower-order eigenvectors and eigenvalues, respectively. This method is the conventional PEM, that is, the random displacement response under pseudo excitation is calculated by the modal displacement method (MDM). However, the truncated modes may significantly affect the results of Eq.(7). Although the MAM can be introduced to reduce the influence of unknown higher-order modes, the error of such responses will increase as the frequency increases [39]. To deal with this problem, we propose a PEM-based method to compute the SPD matrix of random displacement responses under stationary random excitations. This method not only requires less memory space, and also refines computational adaptivity and accuracy.

2.2 Calculation of structural responses based on PEM

The NM for the calculation of frequency responses was first proposed by Wu et al. [38]. As described in Section 2.1, the displacement response $\mathbf{g}_m$ of the system under the m^{th} pseudo

harmonic excitation $\mathbf{B}\boldsymbol{\gamma}_m$ can be obtained by solving the following system:

$$\left(\mathbf{K}+i\omega\mathbf{C}-\omega^2\mathbf{M}\right)\mathbf{g}_m=\mathbf{B}\boldsymbol{\gamma}_m \text{ @}\mathbf{f}_m,\ \omega\in\left[0,\omega_R\right]\ \left(m=1,2,\text{L}\ ,q\right). \tag{8}$$

The proposed method can be used to investigate white-noise excitations with a zero-mean value, i.e., a uniform power spectral density over a given frequency interval. In addition, this method is able to deal with the case of a stationary random excitation $\mathbf{S}_f\left(\omega\right)=\hat{\mathbf{S}}_f\theta\left(\omega\right)$, which can be obtained by applying a filtered white noise model [31] where $\hat{\mathbf{S}}_f$ is a PSD matrix of white-noise excitations and $\theta\left(\omega\right)$ is a real non-negative scalar function. According to Eq.(5), the pseudo excitation can be presented as $\mathbf{f}_m=\sqrt{\theta\left(\omega\right)}\hat{\mathbf{f}}_m$ where $\hat{\mathbf{f}}_m$ does not depend on ω. Based on the modal superposition method, the pseudo harmonic response $\mathbf{g}_m$ in Eq.(8) can be expressed as

$$\mathbf{g}_m\left(\omega\right)=\mathbf{H}\left(\omega\right)\mathbf{f}_m=\boldsymbol{\Phi}\left[\boldsymbol{\Lambda}+i\omega\left(\alpha\mathbf{I}+\beta\boldsymbol{\Lambda}\right)-\omega^2\mathbf{I}\right]^{-1}\boldsymbol{\Phi}^{\text{T}}\mathbf{f}_m. \tag{9}$$

For a large-scale problem, it is unaffordable to compute all modes. It is necessary to quantitatively determine the number of lower-order modes to effectively control the computational time of eigenvalues and its corresponding eigenvectors. So, the Sturm sequence [40] is used to determine l, the number of eigenfrequencies and eigenvectors involved in mode superposition. The following decomposition is first completed

$$\mathbf{K}-\omega_c^2\mathbf{M}=\mathbf{L}\mathbf{D}_c\mathbf{L}^{\text{T}} \tag{10}$$

where

$$\omega_c{}^2=\omega_R{}^2\sqrt{\frac{1+\alpha^2/\omega_R{}^2}{1+\beta^2\omega_R{}^2}}. \tag{11}$$

Then, $l=n_c+1$ can be determined where n_c is the number of negative elements in $\mathbf{D}_c$.

Equation (9) can be further re-written as

$$\mathbf{g}_m=\boldsymbol{\Phi}_{\text{L}}\text{%}_m+\boldsymbol{\Phi}_{\text{H}}\mathbf{c}_m \tag{12}$$

where $\boldsymbol{\Phi}_{\text{L}}=\left[\boldsymbol{\varphi}_1,\text{L}\ ,\boldsymbol{\varphi}_l\right]$ and $\boldsymbol{\Phi}_{\text{H}}$ are matrices composed of the unknown higher-order eigenvectors, $\text{%}_m=\left[\boldsymbol{\Lambda}_{\text{L}}+i\omega\left(\alpha\mathbf{I}_{\text{L}}+\beta\boldsymbol{\Lambda}_{\text{L}}\right)-\omega^2\mathbf{I}_{\text{L}}\right]^{-1}\boldsymbol{\Phi}_{\text{L}}^{\text{T}}\mathbf{f}_m$. The unknown part of $\mathbf{g}_m$ can be written as

$\mathbf{w}_m = \mathbf{\Phi}_{\mathrm{H}}\mathbf{c}_m$ and it satisfies the following equation

$$\begin{aligned}\left[\left(1+i\beta\omega\right)\mathbf{K}+\left(i\alpha\omega-\omega^2\right)\mathbf{M}\right]\mathbf{w}_m\left(\omega\right) &= \mathbf{f}_m-\left[\left(1+i\beta\omega\right)\mathbf{K}+\left(i\alpha\omega-\omega^2\right)\mathbf{M}\right]\mathbf{\Phi}_{\mathrm{L}}\mathbf{p}_m\left(\omega\right)\\ &\equiv \mathbf{f}_m-\mathbf{M}\mathbf{\Phi}_{\mathrm{L}}\mathbf{\Phi}_{\mathrm{L}}^{\mathrm{T}}\mathbf{f}_m,\quad \omega\in\left[0,\omega_R\right]\end{aligned}. \tag{13}$$

The NM [38] is introduced to calculate solutions to Eq.(8) by using Eqs.(12) and (13). Based on the orthogonality of the eigenvectors, Eq.(13) can be transformed to the following equation without changing solutions

$$\left\{\mathbf{K}-\left(\frac{\omega^2-i\alpha\omega}{1+i\beta\omega}\right)\left[\mathbf{M}-\mathbf{M}\mathbf{\Phi}_{\mathrm{L}}\left(\mathbf{M}\mathbf{\Phi}_{\mathrm{L}}\right)^{\mathrm{T}}\right]\right\}\hat{\mathbf{w}}_m\left(\omega\right)=\left(\frac{1}{1+i\beta\omega}\right)\left(\mathbf{f}_m-\mathbf{M}\mathbf{\Phi}_{\mathrm{L}}\mathbf{\Phi}_{\mathrm{L}}^{\mathrm{T}}\mathbf{f}_m\right),\quad \omega\in\left[0,\omega_R\right]. \tag{14}$$

Eq.(14) has a unique solution, and it is the same as that given in Eq.(13). For a detailed proof, we refer readers to Refs [38] and [41].

An iterative method is then applied to obtain the solution of Eq.(14). The linear system in Eq.(14) is first converted into a related system to generate a sequence that can converge to the solution to Eq.(14):

$$\mathbf{w}_m=\mathbf{G}\left(\omega\right)\mathbf{w}_m+\mathbf{p}_m,\ \omega\in\left[0,\omega_R\right] \tag{15}$$

where

$$\mathbf{G}\left(\omega\right)=\left(\frac{\omega^2-i\alpha\omega}{1+i\beta\omega}\right)\mathbf{K}^{-1}\left[\mathbf{M}-\mathbf{M}\mathbf{\Phi}_{\mathrm{L}}(\mathbf{M}\mathbf{\Phi}_{\mathrm{L}})^{\mathrm{T}}\right],\ \mathbf{p}_m=\left(\frac{1}{1+i\beta\omega}\right)\mathbf{K}^{-1}\left(\mathbf{f}_m-\mathbf{M}\mathbf{\Phi}_{\mathrm{L}}\mathbf{\Phi}_{\mathrm{L}}^{\mathrm{T}}\mathbf{f}_m\right). \tag{16}$$

The present choice is motivated by the potential availability of the factorization $\mathbf{K}=\mathbf{U}^{\mathrm{T}}\mathbf{U}$ from the computation of the eigenvectors and eigenvalues [42, 43]. According to Ref. [38], the spectral radius $\rho\left(\omega\right)$ of the iteration matrix $\mathbf{G}\left(\omega\right)$ is a monotonically increasing function of ω in $\left[0,\omega_R\right]$ and its maximum within the interval is $\rho\left(\omega_R\right)=\omega_c^2/\omega_{l+1}^2$, which is smaller than 1 based on Eq.(11). It is worth noting that this method can adaptively determine the number of lower-order modes according to the maximum value of the spectrum radius, thereby accelerating the convergence speed of the iterative algorithm. Therefore, the iterations $\mathbf{w}_m^{(k)}$ defined by

$$\mathbf{w}_m^{(k+1)}=\mathbf{G}\left(\omega\right)\mathbf{w}_m^{(k)}+\mathbf{p}_m,\ \ k=0,1,2,\mathrm{L}\ ,\quad \omega\in\left[0,\omega_R\right] \tag{17}$$

can converge to the solution to Eq.(14) for any starting vector $\mathbf{w}_m^{(0)}$ [44].

Furthermore, setting $\mathbf{w}_m^{(0)} = 0$ and using Eq.(17), we have

$$\mathbf{w}_m^{(k+1)}(\omega) = \left\langle \sum_{j=0}^{k} \left\{ \left(\frac{\omega^2 - i\alpha\omega}{1+i\beta\omega} \right) \mathbf{K}^{-1} \left[\mathbf{M} - \mathbf{M}\boldsymbol{\Phi}_{\mathrm{L}} (\mathbf{M}\boldsymbol{\Phi}_{\mathrm{L}})^{\mathrm{T}} \right] \right\}^{j} \right\rangle \mathbf{f}_m, \quad k=0,1,2,\mathrm{L}\ , \quad \omega \in [0, \omega_R] \tag{18}$$

which is a partial sum of the power series of $\left(\omega^2 - i\alpha\omega\right) \big/ \left(1+i\beta\omega\right)$. The spectral radius of the iteration matrix $\mathbf{G}(\omega)$ arrives at its maximum value at $\omega = \omega_R$. When the partial sum in Eq.(18) with $\omega = \omega_R$ arrives at a given accuracy of convergence, it is also for all $\omega \in [0, \omega_R)$.

Eq.(15) with $\omega = \omega_R$ can be solved iteratively by choosing zero initial vector. The algorithm attempts to ensure that, at the end of the iteration, the ratio of the corresponding increment to the current approximate solution is smaller than some user-specified tolerance. After the iteration algorithm is performed, the corresponding coefficient vectors $\mathbf{p}_m^i \ (i = 0,1,\mathrm{L}\ ,k)$ are determined. Finally, an approximate solution to Eq.(13) can be represented by

$$\mathbf{w}_m^{(k+1)}(\omega) = \frac{1}{1+i\beta\omega} \sum_{j=0}^{k} a^j \mathbf{p}_m^j, \ a = \left(\frac{\omega^2 - i\alpha\omega}{1+i\beta\omega} \right) \Bigg/ \left(\frac{\omega_R^2 - i\alpha\omega_R}{1+i\beta\omega_R} \right), \ \omega \in [0, \omega_R]. \tag{19}$$

Note that the present method is an adaptive one, the number $k+1$ of the coefficient vectors $\mathbf{p}_m^0, \mathbf{p}_m^1, \mathrm{L}\ , \mathbf{p}_m^k$ in the sum Eq.(19) depends on the tolerance error in the iteration algorithm. Based on Eqs.(12) and (19), the approximate solution to Eq.(8) can be written as

$$\mathbf{g}_m^a(\omega) \approx \boldsymbol{\Phi}_{\mathrm{L}} \mathbf{y}_m(\omega) + \mathbf{P}_m \mathbf{z}(\omega), \quad \omega \in [0, \omega_R] \tag{20}$$

where

$$\mathbf{P}_m = \left[\mathbf{p}_m^0, \mathbf{p}_m^1, \mathrm{L}\ , \mathbf{p}_m^k \right], \ \mathbf{z}(\omega) = a_0 \left(1, a, a^2, \mathrm{L}\ , a^k\right)^{\mathrm{T}}, a_0 = \frac{1}{1+i\beta\omega}. \tag{21}$$

The matrices $\boldsymbol{\Phi}_{\mathrm{L}}$ and $\mathbf{P}_m$ are independent of ω, while $\mathbf{y}_m$ and $\mathbf{P}_m$ are functions of ω. The pseudo harmonic response $\mathbf{g}_m$ in Eq.(9) can be computed by using Eqs.(19)-(21) and changing the excitation frequency ω only. For multi-input cases, one only needs to perform an iteration algorithm to obtain the matrix $\mathbf{P}_m$ for different pseudo excitations, this is not time-consuming. Finally, the following relative residual error (RRE) can be used to measure the accuracy of the

proposed method.

$$\varepsilon(\omega)=\sum_{m=1}^{q}\frac{\left\|\left(\mathbf{K}+i\omega\mathbf{C}-\omega^2\mathbf{M}\right)\mathbf{g}_m(\omega)-\mathbf{f}_m\right\|_2}{\left\|\mathbf{f}_m\right\|_2},\ \omega\in[0,\ \omega_R]. \tag{22}$$

3. Topology optimization scheme

The formulation of structural topology optimization under stationary random excitations can be stated as follows:

$$\begin{aligned}&\text{Find}\quad 0<\rho_{\min}\le\rho_e\le 1\ \left(e=1,2,...,n_e\right)\\&\min\quad c\left(\rho_e\right)\\&\text{s.t.}\quad \sum_{e=1}^{n_e}\rho_e v_e\le aV_0\end{aligned} \tag{23}$$

where ρ_e is the artificial density of the element e and it is a design variable in the problem, $\rho_{\min}=0.001$ is the lower bound of the design variables to prevent the occurrence of singularity in the stiffness and mass matrices, v_e is the volume of the element e, V_0 is the total volume of the admissible design domain, a denotes the volume fraction and n_e represents the total number of elements. The objective function c is the integration of the PSD value of concerned DOFs r over a given frequency interval $[0,\omega_R]$:

$$c=\int_0^{\omega_R}S_{u_r}(\omega)d\omega \tag{24}$$

where S_{u_r} is the PSD value of random displacement of concerned DOFs r and can be written as follow as

$$S_{u_r}=\sum_{m=1}^{q}\overline{g}_m^r g_m^r=\sum_{m=1}^{q}\left\|g_m^r\right\|^2 \tag{25}$$

where the superscript r refers to the r^{th}-value of the structural random response vector $\mathbf{g}_m$ and $\overline{g}_m^r$ is the complex conjugate of g_m^r.

The integral of Eq.(24) can be calculated by using the Gauss-Legendre integration rule:

$$\int_0^{\omega_R} S_{u_r}(\omega)\, d\omega = \sum_{k=1}^{N} \gamma_k S_{u_r}(\mu_k) \tag{26}$$

where γ_k is the weighting factor for the k^{th} Gaussian point, μ_k is the Gaussian frequency point, and N is the total number of Gaussian frequency points over the frequency interval $[0, \omega_R]$. For details, readers may refer to Ref.[9].

Structural topology optimization problems are basically a "0 – 1" discrete optimization problem. It will make the objective functions of sequential programming methods, which are widely used in structural optimization, non-differentiable. Hence, Bendsøe [45] introduced a continuous design variable (i.e., the artificial density of an element) and proposed the SIMP interpolation scheme. The classical SIMP method has been widely used in the topology optimization of structures under static load conditions. However, for the topology optimization of structural dynamic problems based on the classical SIMP method, the phenomena of local modes may occur in the sub-regions of a design domain with a low value of the artificial density (e.g., $\rho_e \le 0.1$). This is because the ratio of stiffness to mass is very small in such sub-regions. Some interpolation schemes were proposed to avoid the appearance of localized modes to certain degrees [4, 5, 46, 47]. In this paper, the polynomial interpolation scheme (PIS) [47] is used

$$\begin{aligned} \mathbf{k}_e &= \frac{15\rho_e^5 + \rho_e}{16}\mathbf{k}_{e0} \\ \mathbf{m}_e &= \rho_e \mathbf{m}_{e0} \end{aligned} \tag{27}$$

where $\mathbf{k}_e$ and $\mathbf{m}_e$ are the element stiffness and mass matrices, respectively. $\mathbf{k}_{e0}$ and $\mathbf{m}_{e0}$ denote the corresponding stiffness and mass matrices of the solid element e, respectively.

Sensitivity analysis assumes that external excitations are independent of design variables. The adjoint method [48-51] is chosen herein to compute the sensitivity of objective functions. The method is preferred for the case that the number of design variables is large. In addition, it can also avoid computing eigenvector derivatives, as this is a difficult task in the direct differentiation method. Hence, the derivative of the objective function in Eq.(23) is given by

$$\frac{\partial c}{\partial \rho_e}=\int_0^{\omega_R}\frac{\partial S_{u_r}(\omega)}{\partial \rho_e}d\omega=\int_0^{\omega_R}\left(\sum_{m=1}^{q}2\left\|g_m^r\right\|\frac{\partial\left\|g_m^r\right\|}{\partial \rho_e}\right)d\omega \tag{28}$$

where

$$\frac{\partial\left\|g_m^r\right\|}{\partial \rho_e}=\frac{\overline{g}_m^r\frac{\partial g_m^r}{\partial \rho_e}+g_m^r\frac{\partial \overline{g}_m^r}{\partial \rho_e}}{2\left\|g_m^r\right\|}. \tag{29}$$

As a result, we have

$$\frac{\partial c}{\partial \rho_e}=\int_0^{\omega_R}\sum_{m=1}^{q}\left[\overline{g}_m^r\frac{\partial g_m^r}{\partial \rho_e}+g_m^r\frac{\partial \overline{g}_m^r}{\partial \rho_e}\right]d\omega \tag{30}$$

in which $\frac{\partial g_m^r}{\partial \rho_e}$ can be derived by

$$\frac{\partial g_m^r}{\partial \rho_e}=\frac{\partial\left(\mathbf{L}^{\mathrm{T}}\mathbf{g}_m\right)}{\partial \rho_e}=\mathbf{L}^{\mathrm{T}}\frac{\partial \mathbf{g}_m}{\partial \rho_e} \tag{31}$$

where the vector $\mathbf{L}$ is a column vector with the value of "1" at the r^{th} component and "0" otherwise which r represents the concerned DOFs.

Differentiating Eq.(8) with respect to ρ_e gives

$$\frac{\partial \mathbf{S}}{\partial \rho_e}\mathbf{g}_m+\mathbf{S}\frac{\partial \mathbf{g}_m}{\partial \rho_e}=0 \tag{32}$$

where $\mathbf{S}=\mathbf{K}+i\omega\mathbf{C}-\omega^2\mathbf{M}$ is defined as the dynamic stiffness matrix [40]. Using Eq.(32) and Eq.(31) results in the sensitivity based on the symmetry of $\mathbf{S}$

$$\frac{\partial g_m^r}{\partial \rho_e}=\mathbf{L}^{\mathrm{T}}\frac{\partial \mathbf{g}_m}{\partial \rho_e}=-\mathbf{L}^{\mathrm{T}}\mathbf{S}^{-1}\frac{\partial \mathbf{S}}{\partial \rho_e}\mathbf{g}_m=-\boldsymbol{\lambda}^{\mathrm{T}}\frac{\partial \mathbf{S}}{\partial \rho_e}\mathbf{g}_m \tag{33}$$

in which $\boldsymbol{\lambda}$ is the solution to the following system

$$\mathbf{S}\boldsymbol{\lambda}=\mathbf{L} \tag{34}$$

where the adjoint vector $\boldsymbol{\lambda}$ can be obtained by using the NM introduced in Section 2. Substituting Eq.(33) into Eq.(30) yields the results for sensitivity analysis as follows

$$\frac{\partial c}{\partial \rho_e}=\int_0^{\omega_R}\sum_{m=1}^{q}\left[\overline{g}_m^r\left(-\boldsymbol{\lambda}^{\mathrm{T}}\frac{\partial \mathbf{S}}{\partial \rho_e}\mathbf{g}_m\right)+g_m^r\left(\overline{-\boldsymbol{\lambda}^{\mathrm{T}}\frac{\partial \mathbf{S}}{\partial \rho_e}\mathbf{g}_m}\right)\right]d\omega. \tag{35}$$

In topology optimization, using the artificial density method may induce numerical instability [52], such as checkerboard patterns and mesh-dependencies. A filtering technique proposed by Sigmund [53] can be used to avoid encountering this problem. Finally, the GCMMA algorithm [54] is applied as an optimizer to solve the topology optimization of structures under stationary random excitations. In this paper, for the implementation of the GCMMA algorithm [55, 56], we set

$$\begin{aligned} asyinit &= 0.01 \\ move &= 0.01 \end{aligned} \tag{36}$$

to get more conservative approximations. This selection can avoid running too many inner iterations of GCMMA in some outer iterations and converge to a better performance of optimized structures. Here, the first parameter "*asyinit*" is used to control the rule for updating the lower and upper asymptotes in the first two outer iterations. The second one "*move*" is the move limit of design variables for each outer iteration. Other parameters remain unchanged. A flow chart of the optimization procedures is graphically presented in Fig.1 for illustration.

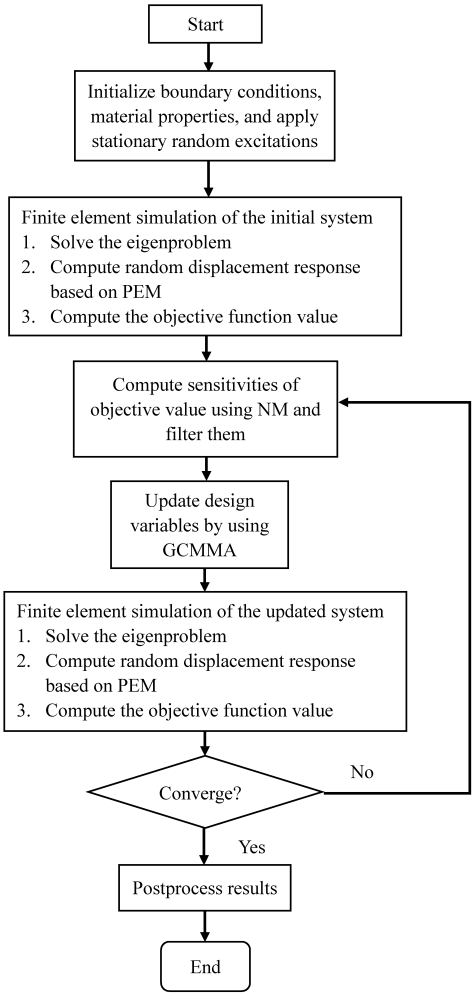

Fig.1. Flow chart of the optimization procedures

4. Numerical examples

In this section, two illustrative examples are given to examine the accuracy and efficiency of the proposed topological optimization scheme. Computations of all examples are run on a server with the Intel CPU Xeon E5-2687W v4, 128G RAM. Both stiffness and mass matrices are stored in a compressed sparse row format. All computation codes are programmed in Fortran and compiled by using the Intel Visual Fortran Compiler XE 2015 with the Intel Math Kernel Library 11.2. In all these cases, we set Young's modulus $E = 2\times10^{11}\,\text{Pa}$, Poisson's ratio $\upsilon = 0.3$, mass density $\rho = 7800\ \text{kg}/\text{m}^3$, proportional damping coefficients $\alpha = 10^{-2}s^{-1}$ and $\beta = 10^{-4}s$, and error tolerance $\varepsilon_1 = 10^{-6}$ in the iteration algorithm. The convergence criterion of the optimization procedures is set to be $\frac{\|c_{k+1}-c_k\|}{\|c_k\|} < 10^{-4}$, where c_k is the objective value of the k^{th} step. The subspace iteration method [43] is used to solve the eigenvalue problems of these examples, and its error tolerance is set to be $\varepsilon_2 = 10^{-10}$.

4.1 Example 1

In this example, we consider a doubly clamped beam structure with a design domain of 6 m × 1 m × 0.01m (thickness), see Fig.2. It is meshed by 300×50 2D 4-Node plane stress elements with 30498 DOFs. The volume fraction is constrained to be less than 50% and the filter radius is set to be 2. A white-noise force excitation is applied at the center of the structure with a PSD value of $S = 9\times10^{6}\,\text{N}^2/(\text{rad/s})$. The objective function is the integral of the PSD for the vertical displacement at the loading position over a given frequency interval. Three frequency intervals $[0,50]\,\text{Hz}$, $[0,200]\,\text{Hz}$ and $[0,500]\,\text{Hz}$ are considered.

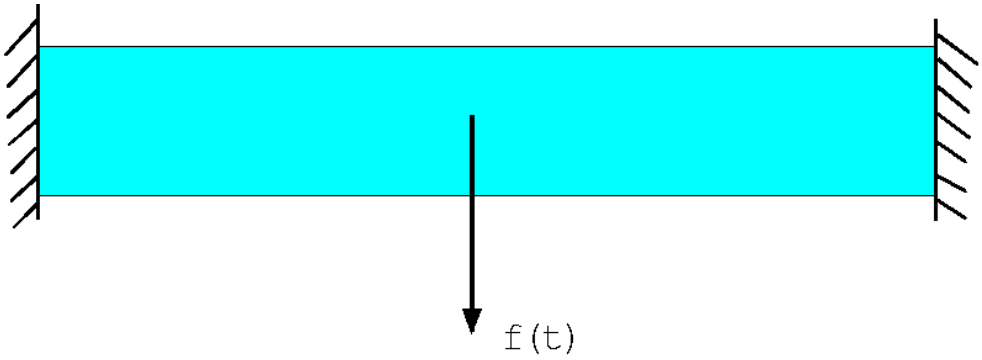

Fig.2 A 2D doubly clamped beam structure

All artificial density values of the initial structure are set to be 0.5. The fundamental natural frequency of the initial structure is 43.1 Hz. The number of natural frequencies of the initial structure within $[0,500]$Hz is 9. The fundamental natural frequencies of the optimized structures for three frequency intervals are 124.8 Hz, 106.8 Hz and 113.5 Hz, respectively. The corresponding optimization history graphs of fundamental natural frequencies for these frequency intervals are plotted in Fig.3. A wider frequency interval does not mean that the optimized structure has a higher fundamental natural frequency, see Fig.3. It is also found that there is no abrupt change in the fundamental natural frequency of the structure during the optimization process. So the phenomenon of localized modes can be remedied by the PIS to certain degrees.

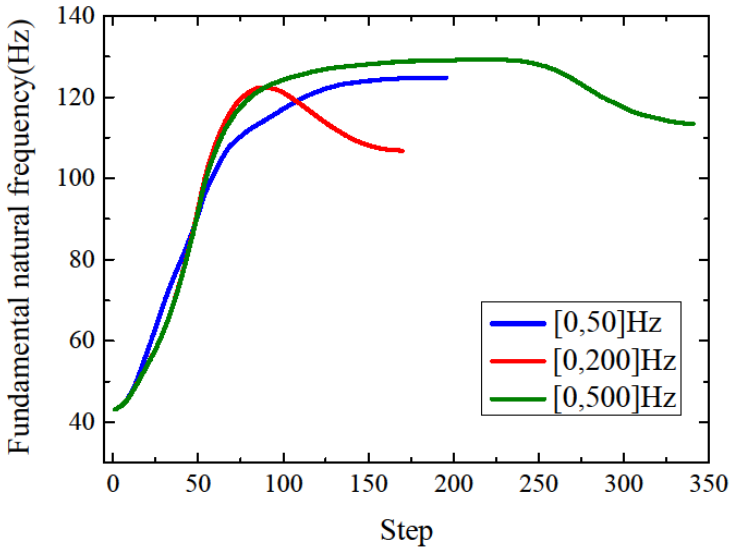

Fig.3 Optimization of the structure for the three frequency intervals in Example 1

Consider the frequency intervals $[0,50]$Hz, $[0,200]$Hz and $[0,500]$Hz, the optimized structures obtained by the proposed topology optimization scheme are shown in Fig.4. Their random responses for the frequency interval $[0,500]$Hz are plotted in Fig.5. The optimized structure under a small frequency interval $[0,\omega_R]$ is similar to the optimized structure under a static load, this is consistent with the conclusion drawn in Ref. [29]. As the frequency interval increases, the effect of dynamic responses may affect the final optimization. The optimization information for these frequency intervals is presented in Table 1, and the corresponding optimization graphs of the objective function values are plotted in Fig.6.

(a) $[0,50]$Hz

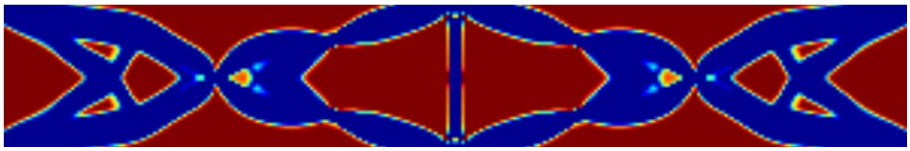

(b) $[0,200]$Hz

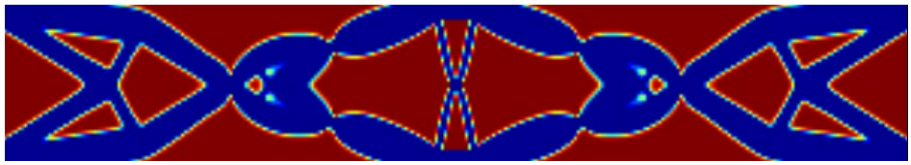

(c) $[0,500]$Hz

Fig.4 Optimized topology designs for the three frequency intervals in Example 1

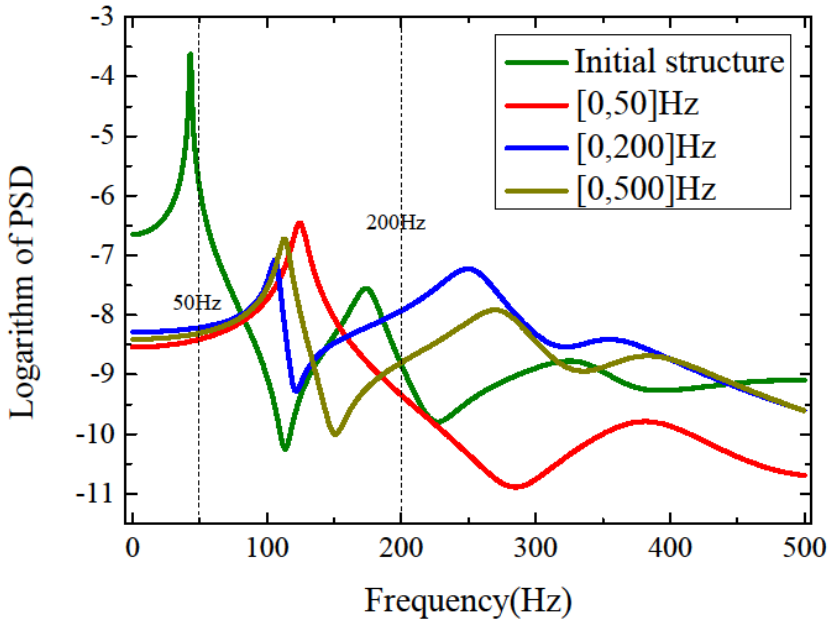

Fig.5 PSD values for the concerned DOFs of the initial and optimized structures in Example 1

Table 1. Performance results of topology optimization based on the proposed scheme for Example 1

	Initial objective value	Converged objective value	Iteration step	CPU time(s)
$[0,50]$ Hz	2.7051e-3	1.0065e-6	196	2731.21
$[0,200]$ Hz	2.7460e-3	1.1719e-5	170	3420.04
$[0,500]$ Hz	2.7475e-3	2.2841e-5	341	17021.84

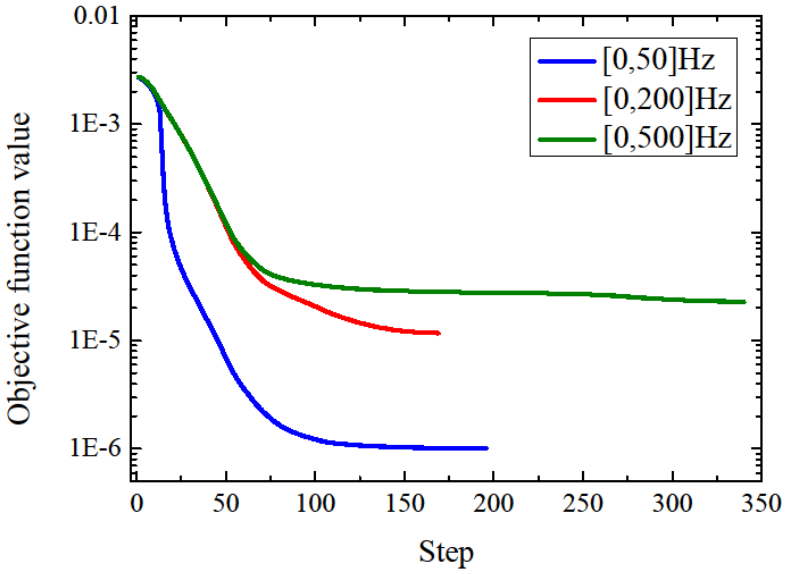

Fig.6 Optimization of the objective function values for the three frequency intervals

The PSD values at the loading position of the initial and optimized structures computed by the FM and NM based on the PEM are shown in Fig.7a for the frequency interval $[0,500]$Hz, this indicates that the responses obtained by using the proposed scheme have a higher accuracy. The corresponding RRE of the random responses calculated by the MDM, MAM and NM based on the PEM, respectively, and the spectral radius of $\mathbf{G}(\omega)$ in Eq.(17) are presented in Fig.7b. Here, 40 lower-order modes are used in MDM and MAM, respectively. It is found that the approximate solutions constructed by applying the iterative algorithm at the maximum point of the spectrum radius satisfy the given accuracy for the whole frequency interval that is consistent with the conclusion drawn in Section 2.2, and the RRE values of structural response vectors are less than $10^{-7.5}$ for the initial structure at all Gaussian frequency points. A higher precision approximate solution makes the converged structure configuration more reliable. On the other hand, we can balance computation effort between the modal analysis and the iteration algorithm by increasing the number of lower modes required for mode superposition. It can reduce the spectral radius $\rho(\omega)$ and make the iteration in Eq.(17) converge faster. The CPU time of computing random responses by the FM and NM based on the PEM at the initial and last steps, and the CPU time distribution of computing frequency responses

by using the NM for the three intervals are all listed in Tables 2–4, respectively. For the frequency intervals $[0,50]$Hz, $[0,200]$Hz and $[0,500]$Hz, the speed-up factors of the NM for the initial and last steps are 16.91 and 5.49, 23.67 and 19.56, and 30.92 and 30.15, respectively. As the number of Gaussian frequency points increases, the speed-up factors also increase.

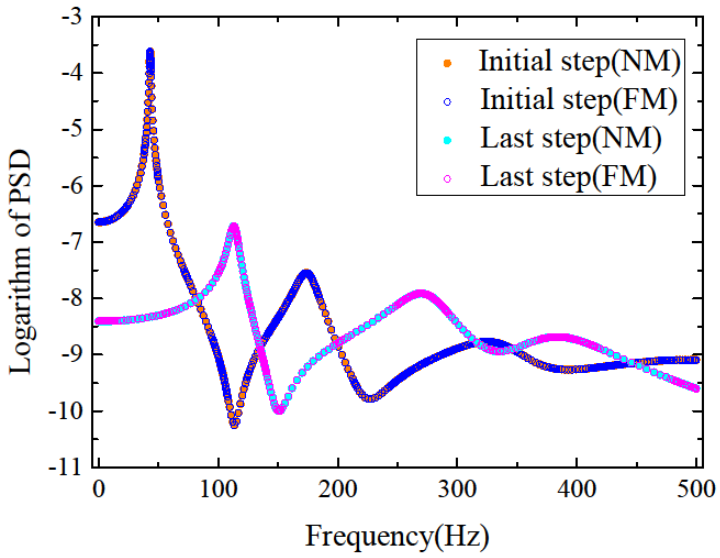

Fig.7a PSD values of user-defined DOFs of the initial and optimized structures computed by FM and NM based on PEM for $[0,500]$Hz in Example 1

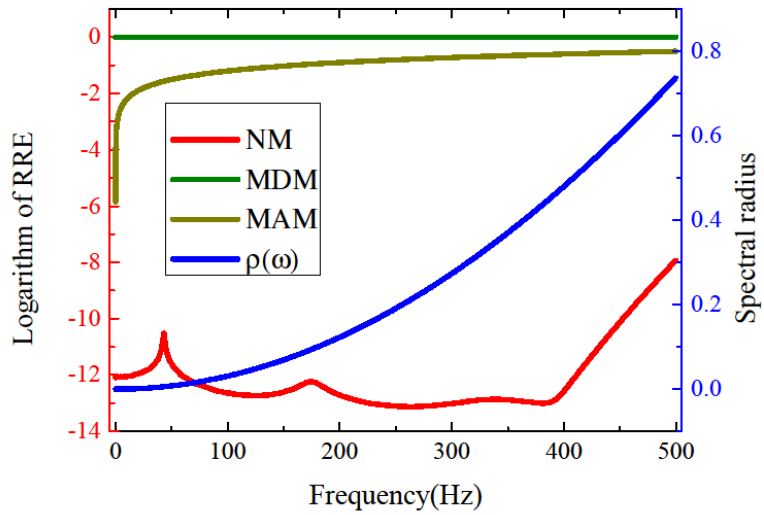

Fig.7b Variation of the spectral radius $\rho(\omega)$ and RRE $\varepsilon(\omega)$ in the frequency interval $[0,500]$Hz for the initial structure

Table 2a. CPU time of computing structural random responses by NM and FM based on PEM at the initial and last steps for Example 1: $[0,50]$Hz

Method	CPU time of initial step (s)	Gaussian frequency points	CPU time of last step (s)	Gaussian frequency points
NM	2.68	144	2.79	48
FM	45.33	144	15.33	48

Table 2b. CPU time distribution of computing structural random responses by NM based on PEM at the initial and last steps for Example 1: $[0,50]$Hz

	Sturm sequence (s)	Number of lower modes	Modal analysis (s)	Iteration algorithm (s)	Number of vectors $\mathbf{p}_m^i$	Solving Eq.(20) (s)	Total (s)
First step	0.64	2	1.17	0.56	7	0.31	2.68
Last step	0.63	1	1.44	0.50	5	0.22	2.79

Table 3a. CPU time of computing structural random response by NM and FM based on PEM at the initial and last steps for Example 1: $[0,200]$Hz

Method	CPU time of initial step (s)	Gaussian frequency points	CPU time of last step (s)	Gaussian frequency points
NM	5.11	432	3.75	256
FM	120.97	432	73.36	256

Table 3b. CPU time distribution of computing structural random responses by NM based on PEM at the initial and last steps for Example 1: $[0,200]$Hz

	Sturm sequence (s)	Number of lower modes	Modal analysis (s)	Iteration algorithm (s)	Number of vectors $\mathbf{p}_m^i$	Solving Eq.(20) (s)	Total (s)
First step	0.60	6	2.03	1.74	14	0.75	5.11
Last step	0.62	5	1.82	0.81	12	0.50	3.75

Table 4a. CPU time of computing structural random responses by NM and FM based on PEM at the initial and last steps for Example 1: $[0,500]$ Hz

Method	CPU time of initial step (s)	Gaussian frequency points	CPU time of converged step (s)	Gaussian frequency points
NM	8.13	928	6.63	736
FM	251.38	928	199.89	736

Table 4b. CPU time distribution of computing structural random responses by NM based on PEM at the initial and last steps for Example 1: $[0,500]$ Hz

	Sturm sequence (s)	Number of lower modes	Modal analysis (s)	Iteration algorithm (s)	Number of vectors $\mathbf{p}_m^i$	Solving Eq.(20) (s)	Total (s)
First step	0.63	10	2.88	2.28	25	2.34	8.13
Last step	0.66	8	2.50	1.56	17	1.91	6.63

4.2 Example 2

In this example, we consider a 3D cantilever structure with a design domain of 0.8 m × 0.4 m × 0.06 m (thickness), as shown in Fig.8. It is meshed by $80\times40\times6$ 3D 8-Node solid elements with 68880 DOFs. The volume fraction is constrained to be 50% and the filter radius is set to be 2. A white-noise force excitation is applied at the center of the right surface with a PSD value of $S=1\times10^{8}\mathrm{N}^2/(\mathrm{rad/s})$. The objective function is the integral of the PSD for the vertical displacement at the loading position over a given frequency interval. Three frequency intervals $[0,100]$ Hz, $[0,500]$ Hz and $[0,1000]$ Hz are taken into account in this study.

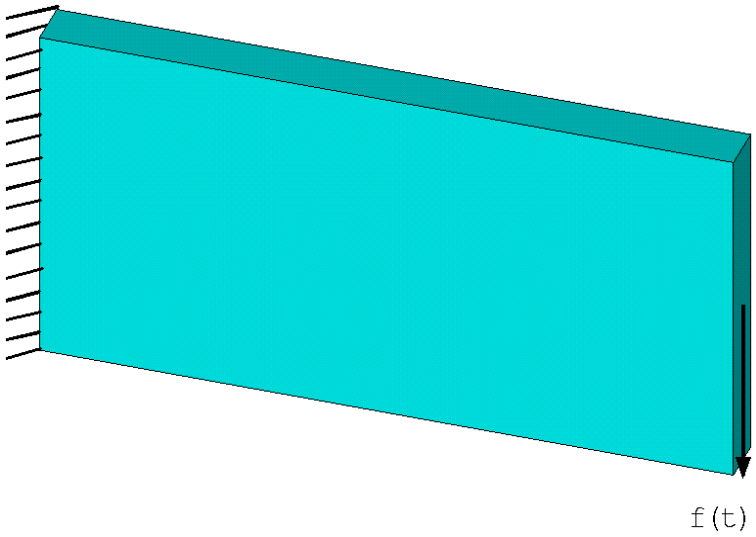

Fig.8 A 3D cantilever structure

This example contains more degrees of freedom and a wider frequency interval to demonstrate the effectiveness of the proposed scheme. All artificial density values of the initial structure are set to be 0.5. The fundamental natural frequency of the initial structure is 27.2 Hz. The number of natural frequencies of the initial structure under $[0,1000]$Hz is 12. The fundamental natural frequencies of the optimized structures for the three frequency intervals are 82.9 Hz, 70.9 Hz and 78.3 Hz, respectively, and their optimization histories are presented in Fig. 9.

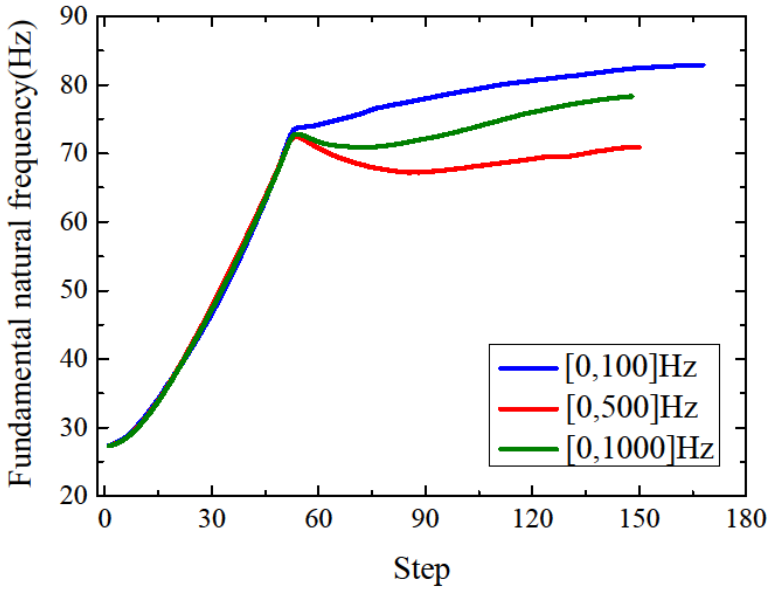

Fig.9 Optimization of the structure for the three frequency intervals

Consider the frequency intervals $[0,100]$ Hz, $[0,500]$ Hz and $[0,1000]$ Hz, the optimized structures acquired by the proposed topology optimization method are presented in Fig.10. Their structural random responses at the frequency interval $[0,1000]$ Hz are given in Fig.11. The optimization details for the three frequency intervals are listed in Table 5, and the corresponding optimization design of the objective function values for the three frequency intervals are shown in Fig.12.

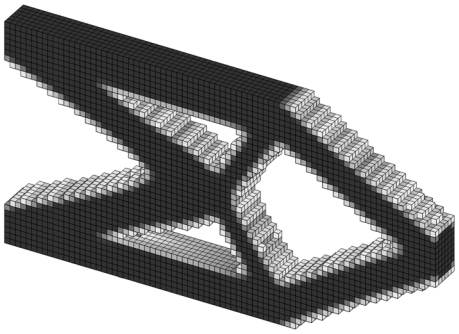

(a) $[0,100]$Hz

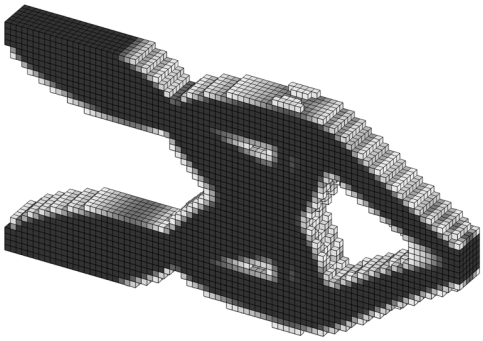

(b) $[0,500]$Hz

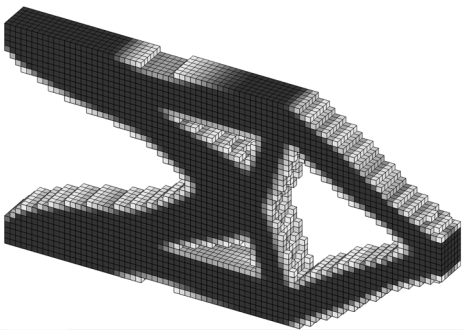

(c) $[0,1000]$Hz

Fig.10 Optimized topology designs for the three frequency intervals in Example 2

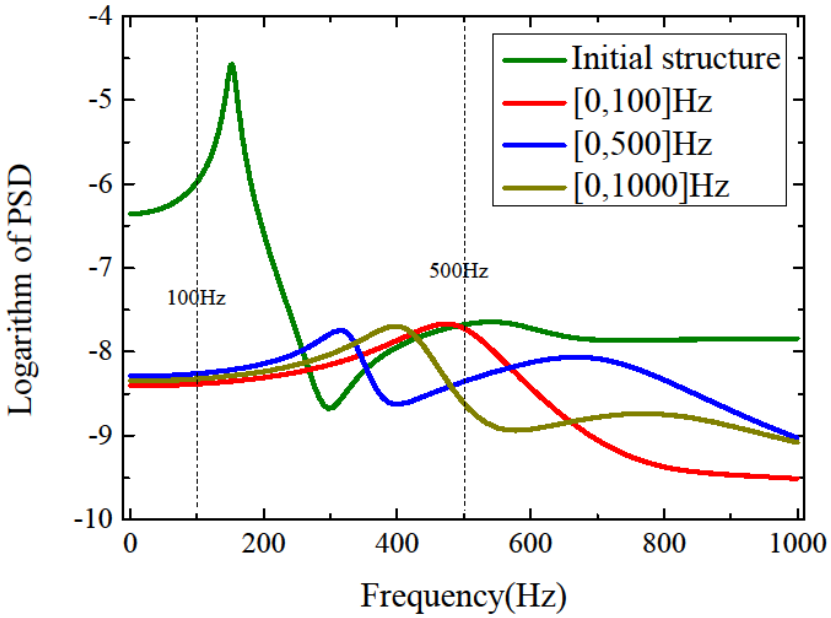

Fig.11 PSD values for the concerned DOFs of the initial and three optimized structures in Example 2

Table 5 Performance results of topology optimization based on the proposed scheme in Example 2

	Initial objective value	Converged objective value	Iteration step	CPU time(s)
$[0,100]$Hz	3.6968e-4	2.5105e-6	168	13904.60
$[0,500]$Hz	3.9517e-3	2.1576e-5	150	36658.47
$[0,1000]$Hz	4.0017e-3	3.0873e-5	148	66579.12

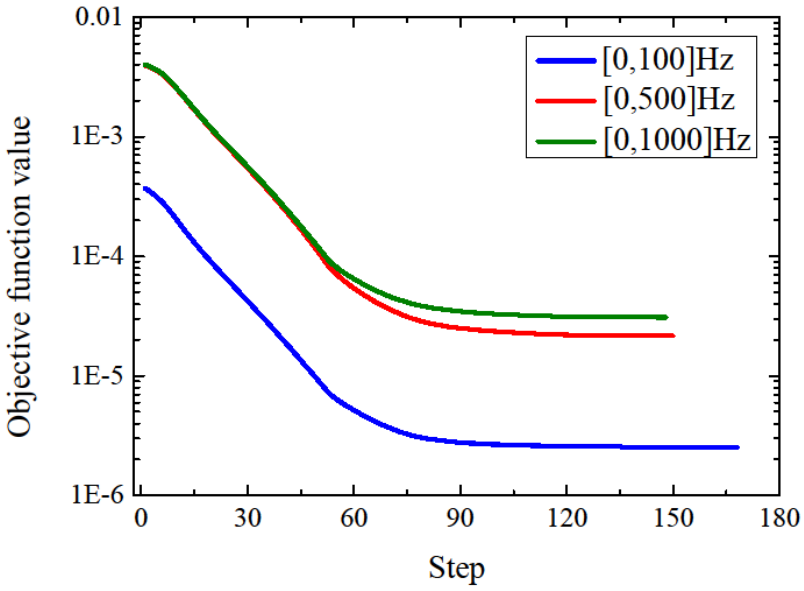

Fig.12 Optimization of the objective function value for the three frequency intervals

In this example, the PSD values at the loading position of the initial and optimized structures computed by the proposed method and exact results are shown in Fig.13a for the frequency interval $[0,1000]$Hz. The corresponding RRE values for the random response vectors computed by the NM based on the PEM and the spectral radius of $\mathbf{G}(\omega)$ are plotted in Fig.13b. In addition, the results of RRE computed by the MDM and MAM based on the PEM using the first 50 lower-order modes of the structure are also plotted in Fig.13b. Fig.13a shows that the proposed method provides a high accuracy approximate solution of structural random responses for the frequency interval. Fig.13b demonstrates that the values of RRE in the response vectors by using the NM based on the PEM are less than 10^{-8} for the initial structures at all Gaussian frequency points.

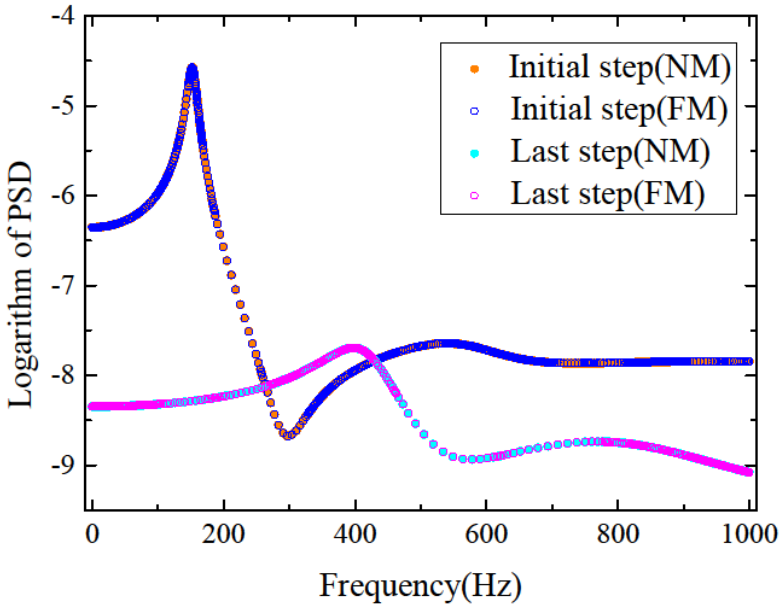

Fig.13a PSD values for the concerned DOFs of the initial and optimized structures computed by FM and NM based on PEM for $[0,1000]$Hz in Example 2

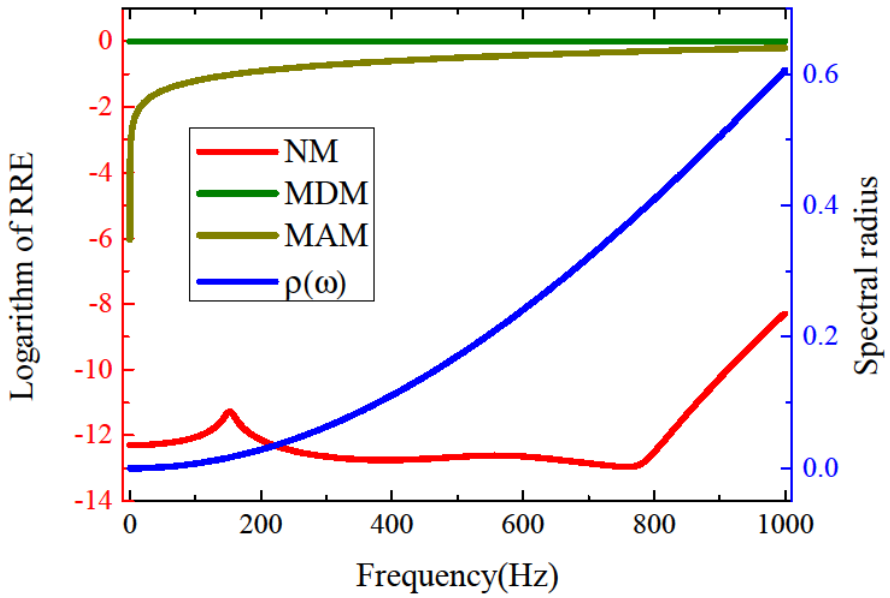

Fig.13b Variation of the spectral radius $\rho(\omega)$ and RRE $\varepsilon(\omega)$ in the frequency interval $[0,1000]$Hz for the initial structure

The CPU time of computing random responses by the FM and NM based on the PEM at the initial and last steps and the CPU time distribution of computing random responses by the NM for all three intervals are all presented in Tables 6–8, respectively. These tables show that for the frequency intervals $[0,100]$Hz $[0,500]$Hz and $[0,1000]$Hz, the speed-up factors of the NM for the initial and last steps are 33.56 and 25.65, 80.46 and 62.90, and 100.64 and 83.75, respectively. We found that the speed-up effect for a 3D problem is more significant than that of the previous example. Furthermore, the speed-up effect is more pronounced as the number of pseudo external excitations increases, because we only need to construct a new convergent series by implementing the iteration algorithm for each external excitation. This step only takes several seconds even for a large-scale problem as shown in Table 8b.

Table 6a CPU time of computing structural random responses by NM and FM based on PEM at the initial and last steps for Example 2: $[0,100]$Hz

Method	CPU time of initial step (s)	Gaussian frequency points	CPU time of last step (s)	Gaussian frequency points
NM	13.30	160	13.08	128
FM	446.38	160	335.56	128

Table 6b CPU time distribution of computing random responses by NM based on PEM at the initial and last steps for Example 2: $[0,100]$Hz

	Sturm sequence (s)	Number of lower modes	Modal analysis (s)	Iteration algorithm (s)	Number of vectors $\mathbf{p}_m^i$	Solving Eq.(20) (s)	Total (s)
First step	3.40	3	6.12	2.70	5	1.08	13.30
Last step	3.36	2	5.78	2.92	6	1.02	13.08

Table 7a CPU time of computing random responses by NM and FM based on PEM at the initial and last steps for Example 2: $[0,500]$Hz

Method	CPU time of initial step (s)	Gaussian frequency points	CPU time of converged step (s)	Gaussian frequency points
NM	20.21	624	17.73	432
FM	1626.19	624	1115.29	432

Table 7b CPU time distribution of computing random responses by NM based on PEM at the initial and last steps for Example 2: $[0,500]$Hz

	Sturm sequence (s)	Number of lower modes	Modal analysis (s)	Iteration algorithm (s)	Number of vectors $\mathbf{p}_m^i$	Solving Eq.(20) (s)	Total (s)
First step	3.76	8	7.30	6.10	9	3.05	20.21
Last step	3.52	5	6.24	5.25	6	2.72	17.73

Table 8a CPU time of computing random responses by NM and FM based on PEM at the initial and last steps for Example 2: $[0,1000]$Hz

Method	CPU time of initial step (s)	Gaussian frequency points	CPU time of converged step (s)	Gaussian frequency points
NM	32.84	1216	28.43	896
FM	3305.09	1216	2380.89	896

Table 8b CPU time distribution of computing random responses by NM based on PEM at the initial and last steps for Example 2: $[0,1000]$Hz

	Sturm sequence (s)	Number of lower modes	Modal analysis (s)	Iteration algorithm (s)	Number of vectors $\mathbf{p}_m^i$	Solving Eq.(20) (s)	Total (s)
First step	3.52	15	12.33	7.36	13	9.63	32.84
Last step	3.36	10	10.12	8.73	15	6.22	28.43

5. Conclusions

This paper presents a new topology optimization procedure for structural random response problems. The proposed scheme that enables trade-offs between computational effort and accuracy is based on the modal superposition and iteration scheme. Compared with the conventional topology optimization method, the present approach possesses higher accuracy and adaptability, which is reflected in three aspects. The first one can adaptively determine the lower-order modes involved in the modal superposition based on the user-defined convergence speed of the iteration algorithm. The second is to compute the structural responses based on a given tolerance error. The last one is able to adjust the computation procedures when updating the design variables. The iteration algorithm only takes a short period of CPU processing time and occupies a small part of memory storage space, even for large-scale structural problems. For multi-input cases, we only need to implement the iteration algorithm for the corresponding systems with different loads. By means of the adjoint method, the sensitivity analysis of the objective function can also be carried out by the NM. Two illustrated examples validate the accuracy and efficiency of the proposed scheme. For the problem of minimizing PSD of random displacements at given DOFs, the topology optimization procedures based on the NM not only increase the computational accuracy but also reduce the CPU time effort remarkably.

In many practical cases, material parameters and applied loads are often random in nature. The proposed method can be extended to compute the statistical moments of structural responses (e.g., mean values and variances) in dynamic reliability-based design optimization. In the future, the topological optimization of engineering structures under non-stationary random excitations will be investigated.

Acknowledgements:

The authors are grateful to Prof. Krister Svanberg from KTH Royal Institute of Technology, Stockholm, for providing the Matlab code of GCMMA optimizer. The work was supported by the National Natural Science Foundation of China (Grant No. 11672118) and the Research Impact Fund (Project No. R5020-18) from the Research Grants Council of Hong Kong.

References

[1] Bendsøe MP, Kikuchi N. Generating optimal topologies in structural design using a homogenization method. Comput Methods Appl Mech Eng. 1988;71:197-224.

[2] Aage N, Andreassen E, Lazarov BS, Sigmund O. Giga-voxel computational morphogenesis for structural design. Nature. 2017;550:84-6.

[3] Zhu JH, Zhang WH, Xia L. Topology optimization in aircraft and aerospace structures design. Arch Comput Methods Eng. 2016;23:595-622.

[4] Pedersen NL. Maximization of eigenvalues using topology optimization. Struct Multidiscip Optim. 2000;20:2-11.

[5] Du JB, Olhoff N. Topological design of freely vibrating continuum structures for maximum values of simple and multiple eigenfrequencies and frequency gaps. Struct Multidiscip Optim. 2007;34:91-110.

[6] Zhao JP, Wang CJ. Dynamic response topology optimization in the time domain using model reduction method. Struct Multidiscip Optim. 2016;53:101-14.

[7] Jeong SH, Lee JW, Yoon GH, Choi DH. Topology optimization considering the fatigue constraint of variable amplitude load based on the equivalent static load approach. Appl Math Model. 2018;56:626-47.

[8] Ma ZD, Kikuchi N, Cheng HC. Topological design for vibrating structures. Comput Methods Appl Mech Eng. 1995;121:259-80.

[9] Liu H, Zhang WH, Gao T. A comparative study of dynamic analysis methods for structural topology optimization under harmonic force excitations. Struct Multidiscip Optim. 2015;51:1321-33.

[10] Liu BS, Huang XD, Huang CF, Sun GY, Yan XL, Li GY. Topological design of structures under dynamic periodic loads. Eng Struct. 2017;142:128-36.

[11] Schuëller GI, Jensen HA. Computational methods in optimization considering uncertainties – An overview. Comput Methods Appl Mech Eng. 2008;198:2-13.

[12] Doltsinis I, Kang Z. Robust design of structures using optimization methods. Comput Methods Appl Mech Eng. 2004;193:2221-37.

[13] Guo X, Bai W, Zhang W, Gao X. Confidence structural robust design and optimization under

stiffness and load uncertainties. Comput Methods Appl Mech Eng. 2009;198:3378-99.

[14] Guo X, Zhang W, Zhang L. Robust structural topology optimization considering boundary uncertainties. Comput Methods Appl Mech Eng. 2013;253:356-68.

[15] Guo X, Zhao X, Zhang W, Yan J, Sun G. Multi-scale robust design and optimization considering load uncertainties. Comput Methods Appl Mech Eng. 2015;283:994-1009.

[16] Wijker J, Copeland TJ. Random Vibrations in Space Structures Design: Theory and Applications. New York: Springer; 2009.

[17] Ma J, Gao W, Wriggers P, Chen J, Sahraee S. Structural dynamic optimal design based on dynamic reliability. Eng Struct. 2011;33:468-76.

[18] Pagnacco E, Lambert S, Khalij L, Rade DA. Design optimisation of linear structures subjected to dynamic random loads with respect to fatigue life. Int J Fatigue. 2012;43:168-77.

[19] Xu JQ, Spencer Jr BF, Lu XL, Chen XZ, Lu L. Optimization of Structures Subject to Stochastic Dynamic Loading. Copmut Aided Civil Infrastruct Eng. 2017;32:657-73.

[20] Fang CJ, Spencer Jr BF, Xu JQ, Tan P, Zhou FL. Optimization of damped outrigger systems subject to stochastic excitation. Eng Struct. 2019;191:280-91.

[21] Rong JH, Xie YM, Yang XY, Liang QQ. Topology optimization of structures under dynamic response constraints. J Sound Vib. 2000;234:177-89.

[22] Rong JH, Tang ZL, Xie YM, Li FY. Topological optimization design of structures under random excitations using SQP method. Eng Struct. 2013;56:2098-106.

[23] Zhang Q, Zhang WH, Zhu JH, Gao T. Layout optimization of multi-component structures under static loads and random excitations. Eng Struct. 2012;43:120-8.

[24] Clough RW, Penzien J. Dynamics of Structures. 2nd ed. New York: McGraw-Hill; 1993.

[25] Zhang WH, Liu H, Gao T. Topology optimization of large-scale structures subjected to stationary random excitation: An efficient optimization procedure integrating pseudo excitation method and mode acceleration method. Comput Struct. 2015;158:61-70.

[26] Lin JH, Zhao Y, Zhang YH. Accurate and highly efficient algorithms for structural stationary/non-stationary random responses. Comput Methods Appl Mech Eng. 2001;191:103-11.

[27] Cornwell RE, Craig RR, Johnson CP. On the application of the mode-acceleration method to

structural engineering problems. Earthq Eng Struct Dyn. 1983;11:679-88.

[28] Zhao L, Xu B, Han YS, Rong JH. Continuum structural topological optimization with dynamic stress response constraints. Adv Eng Softw. 2020;148:102834.

[29] Gomez F, Spencer Jr BF. Topology optimization framework for structures subjected to stationary stochastic dynamic loads. Struct Multidiscip Optim. 2019;59:813-33.

[30] Zhu M, Yang Y, Guest JK, Shields MD. Topology optimization for linear stationary stochastic dynamics: Applications to frame structures. Struct Saf. 2017;67:116-31.

[31] Yang Y, Zhu M, Shields MD, Guest JK. Topology optimization of continuum structures subjected to filtered white noise stochastic excitations. Comput Methods Appl Mech Eng. 2017;324:438-56.

[32] Wu BS, Yang ST, Li ZG, Zheng SP. A preconditioned conjugate gradient method for computing eigenvector derivatives with distinct and repeated eigenvalues. Mech Syst Signal Process. 2014;50:249-59.

[33] Li ZG, Lai S-K, Wu BS. A new method for computation of eigenvector derivatives with distinct and repeated eigenvalues in structural dynamic analysis. Mech Syst Signal Process. 2018;107:78-92.

[34] Alvin KF. Efficient Computation of Eigenvector Sensitivities for Structural Dynamics. AIAA J. 1997;35:1760-6.

[35] Gomez F, Spencer Jr BF, Carrion J. Topology optimization of buildings subjected to stochastic base excitation. Eng Struct. 2020;223:111111.

[36] Benner P, Li J-R, Penzl T. Numerical solution of large-scale Lyapunov equations, Riccati equations, and linear-quadratic optimal control problems. Numer Linear Algebra Appl. 2008;15:755-77.

[37] Yan K, Cheng GD, Wang BP. Adjoint methods of sensitivity analysis for Lyapunov equation. Struct Multidiscip Optim. 2016;53:225-37.

[38] Wu BS, Zhao XQ, Li ZG, Chen X, Zhong HX. An efficient method for calculating the frequency response of a proportional damping system over a given frequency interval. Eng Struct. 2020;220:110987.

[39] Zhao XQ, Wu BS, Li ZG, Zhong HX. A method for topology optimization of structures under harmonic excitations. Struct Multidiscip Optim. 2018;58:475-87.

[40] Bathe K-J. Finite Element Procedures. 2nd ed. Watertown MA: Prentice Hall; 2014.

[41] Wu BS, Yang ST, Li ZG, Zhong HX, Chen X. Computation of frequency responses and their sensitivities for undamped systems. Eng Struct. 2019;182:416-26.

[42] Grimes RG, Lewis JG, Simon HD. A shifted block Lanczos algorithm for solving sparse symmetric generalized eigenproblems. SIAM J Matrix Anal Appl. 1994;15:228-72.

[43] Bathe K-J. The subspace iteration method – Revisited. Comput Struct. 2013;126:177-83.

[44] Golub GH, Van Loan CF. Matrix Computations. 4th ed. Baltimore: Johns Hopkins University Press; 2013.

[45] Bendsøe MP. Optimal shape design as a material distribution problem. Struct Optim. 1989;1:193-202

[46] Stolpe M, Svanberg K. An alternative interpolation scheme for minimum compliance topology optimization. Struct Multidiscip Optim. 2001;22:116-24.

[47] Zhu JH, Beckers P, Zhang WH. On the multi-component layout design with inertial force. J Comput Appl Math. 2010;234:2222-30.

[48] Haftka RT, Gürdal Z. Elements of Structural Optimization. 3rd ed. Dordrecht: Kluwer; 1992.

[49] Bendsøe MP, Sigmund O. Topology Optimization: theory, methods, and applications. 2nd ed. Berlin: Springer; 2004.

[50] Choi KK, Kim NH. Structural Sensitivity Analysis and Optimization. New York: Springer; 2005.

[51] Yan K, Cheng GD. An adjoint method of sensitivity analysis for residual vibrations of structures subject to impacts. J Sound Vib. 2018;418:15-35.

[52] Sigmund O, Petersson J. Numerical instabilities in topology optimization: A survey on procedures dealing with checkerboards, mesh-dependencies and local minima. Struct Optim. 1998;16:68-75.

[53] Sigmund O. On the design of compliant mechanisms using topology optimization. Mech Struct Mach. 1997;25:493-524.

[54] Svanberg K. A class of globally convergent optimization methods based on conservative convex separable approximations. SIAM J Optim. 2002;12:555-73.

[55] Svanberg K. MMA and GCMMA - two methods for nonlinear optimization. 2007. http://www.math.kth.se/~krille/gcmma07.pdf.

[56] Silva OM, Neves MM, Lenzi A. A critical analysis of using the dynamic compliance as objective function in topology optimization of one-material structures considering steady-state forced vibration problems. J Sound Vib. 2019;444:1-20.